Siderophore and indolic acid production by *Paenibacillus triticisoli* BJ-18 and their plant growth-promoting and antimicrobe abilities

Yunzhi Zhang[1], Jinwei Ren[2], Wenzhao Wang[2], Baosong Chen[2], Erwei Li[2] and Sanfeng Chen[1]

[1] State Key Laboratory for Agrobiotechnology, College of Biological Sciences, China Agricultural University, Beijing, People's Republic of China
[2] State Key Laboratory of Mycology, Institute of Microbiology, Chinese Academy of Sciences, Beijing, People's Republic of China

ABSTRACT

Paenibacillus triticisoli BJ-18, a N_2-fixing bacterium, is able to promote plant growth, but the secondary metabolites that may play a role in promoting plant growth have never been characterized. In this study, untargeted metabolomics profiling of *P. triticisoli* BJ-18 indicated the existence of 101 known compounds, including N^2-acetyl ornithine, which is the precursor of siderophores, plant growth regulators such as trehalose 6-phosphate, betaine and trigonelline, and other bioactive molecules such as oxymatrine, diosmetin, luotonin A, (-)-caryophyllene oxide and tetrahydrocurcumin. In addition, six compounds were also isolated from *P. triticisoli* BJ-18 using a combination of silica gel chromatography, sephadex LH-20, octadecyl silane (ODS), and high-performance liquid chromatography (HPLC). The compound structures were further analyzed by Nuclear Magnetic Resonance (NMR), Mass Spectrometry (MS), and Electronic Circular Dichroism (ECD). The six compounds included three classical siderophore fusarinines identified as deshydroxylferritriacetylfusigen, desferritriacetylfusigen, and triacetylfusigen, and three indolic acids identified as paenibacillic acid A, 3-indoleacetic acid (IAA), and 3-indolepropionic acid (IPA). Both deshydroxylferritriacetylfusigen and paenibacillic acid A have new structures. Fusarinines, which normally occur in fungi, were isolated from bacterium for the first time in this study. Both siderophores (compounds **1** and **2**) showed antimicrobial activity against *Escherichia coli, Staphylococcus aureus* and *Bacillus subtilis*, but did not show obvious inhibitory activity against yeast *Candida albicans*, whereas triacetylfusigen (compound **3**) showed no antibiosis activity against these test microorganisms. Paenibacillic acid A, IAA, and IPA were shown to promote the growth of plant shoots and roots, and paenibacillic acid A also showed antimicrobial activity against *S. aureus*. Our study demonstrates that siderophores and indolic acids may play an important role in plant growth promotion by *P. triticisoli* BJ-18.

Subjects Agricultural Science, Biochemistry, Microbiology
Keywords *Paenibacillus triticisoli* BJ-18, Siderophore, Fusarinine, Indolic acid

INTRODUCTION

Plant growth-promoting bacteria (PGPB) have great usage as agricultural inoculants, such as biofertilization and biocontrol of pathogens (*Backer et al., 2018*). Commercialized PGPB strains mainly include the members of *Agrobacterium, Azospirillum, Bacillus, Paenibacillus, Pseudomonas, Streptomyces* et al. (*Lucy, Reed & Glick, 2004*; *Banerjee et al., 2006*). PGPB may promote plant growth directly usually by either facilitating resource acquisition (e.g., nitrogen fixation, production of indolic compounds and siderophores, phosphate solubilization, and 1—aminocyclopropane—1—carboxylate deaminase activity) or indirectly by decreasing the inhibitory effects of various pathogenic agents on plant growth and development (antibiotics and lytic enzymes); that is, by acting as biocontrol bacteria (*Glick, 2012*).

Nitrogen (N) fixation is catalyzed by molybdenum-dependent nitrogenase, which is a metalloenzyme composed of two protein components, referred to as MoFe protein and Fe protein. The atmospheric N_2 is reduced to bioavailable NH_4^+ by nitrogen fixation, providing a large amount of natural N into cultivated agricultural systems (*Galloway et al., 2008*). In addition to symbiotic N_2-fixing *Rhizobia* associated with legumes, the non-symbiotic N_2-fixing bacteria are also important contributors to the N nutrition of non-legumes (*Gupta, Roper & Roget, 2006*). It is estimated that the microbial N accounts for roughly 30–50% of the total N in crop fields (*Liu et al., 2017*).

Iron is the fourth most abundant element on earth but its bioavailability is extremely limited due to its poor solubility (*Braun & Braun, 2002*; *Miethke & Marahiel, 2007*; *Kazamia et al., 2018*). Microbes have evolved strategies to obtain sufficient amounts of iron, such as chelation, reduction, and protonation (*Guerinot, 1994*). The use of a siderophore to transport iron by chelation is vitally important for bacteria. Siderophores are low molecular weight compounds (500–1,500 Da) possessing a high affinity for Fe^{3+} ($K_f > 10^{30}$) (*Haas & Defago, 2005*) and they are synthesized by bacteria through non-ribosomal pathways (*Hutchins et al., 1999*; *Khan et al., 2020*). Many PGPB have been reported to produce siderophores, such as *Bacillus subtilis*, *Paenibacillus polymyxa* SK1, *Mesorhizobium* sp., *Brevibacillus brevis* GZDF3 (*Franco-Sierra et al., 2020*; *Khan et al., 2020*; *Menéndez et al., 2020*; *Sheng et al., 2020*). The chelate of siderophores and ferric iron can be directly absorbed by plants and are called mechanism III, which is thought to be used by plants to resist iron stress (*Shenker et al., 1992*; *Yehuda et al., 1996*; *Chen, Dick & Streeter, 2000*). When grown under iron-limiting conditions, mung bean plants by inoculation with the siderophore-producing *Pseudomonas* strain GRP3 showed reduced chlorotic symptoms and an enhanced chlorophyll level compared to uninoculated plants (*Sharma et al., 2003*). Tomato seedlings inoculation with these two *Mesorhizobium* strains that produce siderophores and IAA showed significantly higher plant growth traits than uninoculated seedlings (*Menéndez et al., 2020*). In addition, siderophores secreted by PGPB can suppress plant pathogens by competing for trace amounts of iron in the environment (*Glick, 2012*). It has been suggested that biocontrol PGPB produce siderophores that have a much greater affinity for iron than do fungal pathogens so that the fungal pathogens are unable to proliferate in the root rhizosphere of the host plant due to lack of iron (*Schippers, Bakker*

& *Bakker, 2003*; *O'Sullivan & O'Gara, 1992*). For examples, siderophores have biocontrol roles against plant pathogens, such as *Pirycularia oryzae* (*Yuquan et al., 1999*), *Stagonospora curtisii* (*Shuangya, Yongxiang & Xiangqun, 2003*), *Fusarium oxysporum* (*Duijff et al., 1993*), *Macrophomina phaseolina* (*Arora, Kang & Maheshwari, 2001*) and *Cryphonectria parasitica* (*Chen et al., 2006*).

Indolic acids include several compounds, of which indole-3-acetic acid (indole acetic acid, IAA) is by far the most common as well as the most studied auxin (*Xie et al., 2005*). They stimulate cell division and promote cell elongation (*Katzy et al., 1990*; *Weyers & Paterson, 2001*). They are abundant in higher plants and rhizospheric microorganisms and play a vital role in plant–microbe interactions (*Beneduzi et al., 2008*; *Costacurta & Vanderleyden, 1995*; *Lambrecht et al., 2000*; *Beck, Hansen & Lauritsen, 2003*; *Mao et al., 2014*). Previous studies have demonstrated that *Paenibacillus* spp. can produce indolic compounds to promote plant growth (*Kumari & Thakur, 2018*; *Castellano et al., 2018*; *Lebuhn, Heulin & Hartmann, 1997*). Endophytic bacteria promote growth of the medicinal legume *Clitoria ternatea* by IAA production, P and K-solubilization (*Aeron, Maheshwari & Meena, 2020*).

Paenibacillus triticisoli BJ-18 (=DSM 25425^T = CGMCC 1.12045^T) is a N$_2$-fixing bacterium isolated by our laboratory from wheat rhizosphere soil in Beijing (*Wang et al., 2013*). Recently, we have shown that inoculation with *P. triticisoli* BJ-18 significantly promotes the growth of tomato, maize and wheat (*Xie et al., 2016*; *Shi et al., 2016*; *Li et al., 2019*). The ^{15}N-isotope-enrichment experiment indicated that plant seedlings inoculated with *P. triticisoli* BJ-18 derived 12.9–36.4% N from nitrogen fixation (*Li et al., 2019*). However, the secondary metabolites of *P. triticisoli* BJ-18 have never been isolated or characterized. In this study, six compounds, composed of three siderophores and three indolic acids, were isolated and characterized from *P. triticisoli* BJ-18. Notably, a new siderophore and a new indolic acid were here identified. Our results will provide insight into the mechanisms by which *P. triticisoli* BJ-18 promotes plant-growth, including nitrogen fixation and the secretion of siderophores and indolic acids.

MATERIALS & METHODS

Bacterial strain
The bacterial strain *Paenibacillus triticisoli* BJ-18 (=DSM 25425^T = CGMCC 1.12045^T) was used in our study.

Untargeted metabolomics by LC-MS
The equipment and raw data for untargeted metabolomics were provided by Beijing Novogene Technology Co., Ltd. *P. triticisoli* BJ-18 was cultured in Lysogeny Broth (LB) (10 g tryptone, 5 g yeast, 10 g NaCl, 15 g agar per 1 L H$_2$O) at 30 °C for 3 days. A single colony was inoculated in 20 mL CH medium (30 g sucrose, 6.4 g tryptone, 7 g yeast, 0.6 g MgSO$_4$ · 7H$_2$O, 3.5 g NaCl, 0.1 g K$_2$HPO$_4$, 0.4 g KH$_2$PO$_4$ per 1 L H$_2$O) and cultured at 30 °C 200 rpm for 48 h. The seed solution was inoculated into 150 mL of CH medium at an inoculation amount of 2% and cultured at 30 °C 200 rpm for 48 h. Cells were harvested by centrifugation at 6,000 rpm at 4 °C for 10 min, ground with liquid nitrogen,

and resuspended with 500 µL of 80% methanol solution containing 0.1% formic acid. The homogenate was incubated on ice for 5 min and was centrifuged at 15,000 rpm at 4 °C for 10 min. 200 µL of supernatant was subsequently transferred to a fresh Eppendorf tube with a 0.22 µM filter and was centrifuged at 15,000 rpm at 4 °C for 10 min. LC-MS/MS analyses were performed using the Vanquish UHPLC system (Thermo Fisher) coupled with an Orbitrap Q Exactive series mass spectrometer (Thermo Fisher) in a Hyperil Gold column (100×2.1 mM, 1.9 µM) with a 16-min linear gradient at a flow rate of 0.2 mL/min. The eluents for the positive polarity mode were eluent A (0.1% formic acid in water) and eluent B (methanol). The eluents for the negative polarity mode were eluent A (5 mM ammonium acetate, pH 9.0) and eluent B (methanol). The solvent gradient was set as follows: 2% B, 1.5 min; 2–100% B, 12.0 min; 100% B, 14.0 min;100–2% B, 14.1 min; 2% B, 16 min. The Q exactive mass series spectrometer was operated in positive/negative polarity mode with spray voltage of 3.2 kV, sheath gas flow rate of 35 arb, aux gas flow rate of 10 arb, and a capillary temperature of 320 °C. Compound discoverer 3.0 (CD 3.0, Thermo Fisher) was used for processing the data files to match results from the mzCloud (https://www.mzcloud.org/) and ChemSpider (http://www.chemspider.com/) databases. Accurate qualitative and relative quantitative results were obtained through statistical analysis.

Reagents and instruments for separation and purification of compounds 1-6

HPLC data were acquired using a Waters 2695 instrument. HRESIMS and HPLC-ESI-MS data were obtained using an Accurate-Mass-Q-TOF LC/MS 6520 instrument (Agilent, USA) in positive ion mode. ^{1}H and ^{13}C NMR data were obtained by Bruker Avance-500 spectrometers (Rheinstetten, Germany) with solvent signals (DMSO-d_6, δ_H 2.500/ δ_C 39.520) as references, and HSQC and HMBC experiments were optimized for 145.0 and 8.0 Hz, respectively. The optical rotations measurement was conducted on an Anton Paar MCP200 polarimeter (Anton Paar, Austria). Optical rotations were conducted using a Perkin-Elmer 241 polarimeter, and UV data were detected by a Shimadzu Biospec-1601 spectrophotometer. The absorbance of 96-well clear plate was measured on a microplate reader (Molecular Devices, SpectraMax® Paradigm®). Analytically pure solvents including methanol, dichloromethane, and ethyl acetate were used for extraction and chromatographic separation. TLC was carried out on silica gel HSGF$_{254}$ plates and spots were visualized by UV at 254 nm or sprayed with 10% H_2SO_4 and heated. Silica gel (150 −250 µM, Qingdao Haiyang Chemical Co., Ltd.), octadecylsilyl (ODS, 50 µM, YMC CO., LTD), and Sephadex LH-20 (Amersham Biosciences) were used for column chromatography (CC). HPLC separation was performed on an Agilent 1200 HPLC system with a Diode Array Detector (DAD) detector using an ODS column (C$_{18}$, 250×9.4 mM, YMC Pak, 5 µM) at a flow rate of 2.0 mL/min.

Extraction and isolation of the secondary metabolites

P. triticisoli BJ-18 was grown in a 500 L fermenter (Biotech, Shanghai Baoxing Biological Equipment Engineering Co., Ltd.) filled with 200 L of CH medium at pH 5.0 with 40% to

60% dissolved oxygen and shaking at 100 rpm and at 30 °C for 48 h. For doing this, this bacterium was inoculated into 20 mL of CH medium and then scaled-up to 20 L. The seed culture was inoculated into 200 L of CH medium with an inoculation amount of 1% in a 500 L fermenter.

The fermented culture was passed through a 200 mesh macroporous adsorption resin following 3 periods of 30-minute ultrasonic cell-breaking and was eluted with analytically pure methanol. The organic solvent was collected and evaporated using rotary evaporators to obtain the crude extract (7 g). The aqueous phase was discarded after being extracted and separated three times between the ethyl acetate and the aqueous phases, and the organic phase was retained and evaporated using rotary evaporators. The final product was 4 g of EtOAc (ethyl acetate) extract.

The EtOAc extract was separated into 20 subfractions (Pt-1 to Pt-20) after being subjected to ODS column chromatography with a gradient of methanol-water (5–100%). The fraction Pt-10 was further partitioned by Sephadex LH-20 CC separated by 50% methanol in water to create 26 subfractions (Pt-10-1 to Pt-10-26). Compound **4** (4.2 mg, t_R 31.2 min) was obtained from fraction Pt-10-24 (21.3 mg) by RP-HPLC using 55% methanol in acidic water. Fraction Pt-13 was divided into 16 fractions, Pt-13-1 to Pt-13-16, after being subjected to ODS column chromatography with a gradient of MeOH-H_2O (40–80%). Compounds **1**-**3** (2 mg, 3.1 mg and 8 mg, t_R 62.5 min, 58.4 min and 37.4 min, respectively) were obtained from fractions Pt-13-6 (42.5 mg) by RP-HPLC using 20% acetonitrile in acidic water. Fraction Pt-15 was further partitioned by Sephadex LH-20 CC eluted with 90% methanol in water to cut to 6 subfractions (Pt-15-1 to Pt-15-6). Compound **5** (214 mg, t_R 42.5 min) was obtained from fraction Pt-15-4 (830 mg) by RP-HPLC using 72% methanol in acid water. Compound **6** (37.6 mg, t_R 62.5 min) was isolated from fraction Pb-17 (928 mg) by RP-HPLC (C8) using 80% methanol in acid water.

Deshydroxylferritriacetylfusigen (compound **1**): yellow powder; $[\alpha]^{25}_D = -14.0$ (c 0.10, MeOH); UV (MeOH) λ_{max} (log ε) 214 (2.44) nm; NMR data (500 MHz, DMSO-d_6) is shown in Table 1; positive HRESIMS m/z 837.4242 [M + H]$^+$ (calculated for $C_{39}H_{61}N_6O_{14}$, 837.4246 $\Delta = 0.0004$).

Desferritriacetylfusigen (compound **2**): yellow powder; $[\alpha]^{25}_D = -8.0$ (c 0.05, MeOH); UV (MeOH) λ_{max} (log ε) = 214 (2.43) nm; positive HRESIMS m/z 853.4203 [M + H]$^+$, (calculated for $C_{39}H_{60}N_6O_{15}$, 853.4195 $\Delta = 0.0008$).

Triacetylfusigen (compound **3**): brown powder; $[\alpha]^{25}_D = -216.0$ (c 0.025, MeOH); UV (MeOH) λ_{max} (log ε) 211 (2.35) nm; positive HRESIMS m/z 906.3316 [M + H]$^+$ (calculated for $C_{39}H_{58}N_6O_{15}Fe$, 906.3309 $\Delta = 0.0007$).

Paenibacillic acid A (compound **4**): white powder; $[\alpha]^{25}_D = -39.99$ (c 0.10, MeOH); UV (MeOH) λ_{max} (log ε) 211 (2.33) nm; NMR data (500 MHz, DMSO-d_6) is shown in Table 2; positive HRESIMS m/z 303.1704 [M + H]$^+$ (calculated for $C_{17}H_{23}N_2O_3$ 303.1708 $\Delta = 0.0004$).

3-Indoleacetic acid (IAA) (compound **5**): white amorphous powder; UV (MeOH) λ_{max} (log ε) 234 (4.22), 272 (3.77), 280 (3.80), 290 (3.72) nm; positive HRESIMS m/z 176.0709 [M + H]$^+$ (calculated for $C_{10}H_{10}NO_2$ 176.0701 $\Delta = 0.0008$).

Table 1 NMR data of compound 1 in DMSO-d_6.

Pos.	δ_C[a]	δ_H[b], mult (J in Hz)
1	166.0	
2	117.5	6.31, s
3	150.0	
4	31.9	2.80, br. s
5	63.1	4.17, m
		4.12, m
6	172.1	
7	51.8	4.19, m
8	28.0	1.65, m
9	23.0	1.53, m
10	46.3	3.51 br. s
11	25.3	1.87, s
12	169.5	
13	22.3	1.84, s
N-OH		9.70, br. s
N-H		8.20, d (7.5)

Notes.
[a] Recorded at 125 MHz.
[b] Recorded at 500 MHz.

3-Indolepropionic acid (IPA) (compound **6**): white amorphous powder; UV (MeOH) λ_{max} (log ε) 235(4.25), 270 (3.77), 280 (3.80), 290 (3.72) nm; positive HRESIMS m/z 190.0871 [M + H]$^+$ (calculated for $C_{11}H_{12}NO_2$, 190.0868 $\Delta = 0.0003$).

Conversion of compound 3 into desferritriacetylfusigen

The removal of the ferric ion was conducted as reported by *Kodani et al. (2015)* with additional changes. Compound **3** (4 mg) was dissolved in 1.5 mL of water and then 1.5 mL of 1M 8-quinolinol was added. The solution was stirred for 25 min and mixed with three mL of CH_2Cl_2, then left to stand until bilayer separation occurred. The water layer was evaporated using a freeze-dryer vacuum. This was repeated 3 times to eliminate ferri-8-quinolinol and obtain the total dry material. The sample was then dissolved in 100 μL of methanol and HPLC purification was performed with the C18 column (7.8× 300 mM, Waters, 7 μM; detector: UV), eluted with 20% acetonitrile in water at a flow rate of one mL/min, and monitored at OD_{210} to create 2.0 mg of desferri-compound **3**. Positive HRESIMS and NMR of desferri-compound **3** was the same as compound **2**.

ECD computations

Systematic conformation analysis of 4a were conducted with CONFLEX (version 7 Rev. A; CONFLEX Corporation) using the MMFF94 molecular mechanics force field. Optimization with DFT calculation at the B3LYP/6-31G(d) level in MeOH in methanol with the PCM model using the Gaussian 09 program (Revision C.01, Gaussian Inc.) afforded the MMFF minima. The 40 lowest electronic transitions were calculated using time-dependent density-functional theory (TDDFT) methodology at the B3LYP/6-31G(d) level. The overall ECD

Zhang et al. (2020), *PeerJ*, DOI 10.7717/peerj.9403

6/26

Table 2 NMR data of compound 4 in DMSO-d_6.

Pos.	δ_C [a]	δ_H [b], mult (J in Hz)
1	39.5	4.35, d (15.7)
		4.21, d (15.7)
3	56.1	3.63, dd (10.3, 5.0)
4	22.9	3.13, dd (15.3, 5.0)
		2.84, dd (15.3, 10.4)
4a	108.2	
4b	126.2	
5	118.1	7.47, d (7.5)
6	119.7	7.07, t (7.5)
7	121.9	7.17, t (7.5)
8	109.8	7.55, d (7.5)
8a	137.2	
9a	129.4	
1′	170.0	
2′	72.3	5.46, s
3′	67.1	3.30, m
4′	31.0	1.40, m
5′	18.8	1.22, m
6′	13.6	0.78, t (7.4)

Notes.
[a] Recorded at 125 MHz.
[b] Recorded at 500 MHz.

spectra were then produced based on Boltzmann weighting of each conformer as described in literature(*Liu et al., 2018a*; *Liu et al., 2018b*).

Determination of plant growth promoting capacity of indolic compounds

The seeds of *Arabidopsis thaliana* var. Columbia were sterilized using 75% ethanol for 45 s, 5% NaClO for 15 min, and were washed in sterile water 3 times. The seeds were then placed horizontally on solid 1/2 Murashige and Skoog (MS) (*Murashige & Skoog, 1962*) medium supplemented with 1.5% sucrose, 0.35% (w/v) agar, and different concentrations and combinations of 1 mg/L paenibacillic acid A, IAA, and IPA for direct regeneration. At least ten *Arabidopsis* strains were cultured in each group of treatments. The cultures were incubated at 25 ± 2 °C under cool fluorescent light (2000 lux 16 h/day photoperiod) for 14 days. The ability of the three indolic acids to promote plant growth was evaluated by measuring the dry weight of the stems and roots of *Arabidopsis thaliana*.

Detection of indolic compounds

The Salkowski Reagent (PC technique) was used to determine concentrations of indolic compounds (*Glickmann & Dessaux, 1995*). IAA standard solutions with concentrations of 0, 5.0, 10.0, 15.0, 20.0, and 25.0 µg /mL were used to react with an equal volume of PC reagent in the dark for half an hour and the OD$_{530}$ value was measured to draw the Salkowski calibration curve. The R^2 value should be greater than 0.99.

P. triticisoli BJ-18 was grown overnight in 50 mL of LB medium at 200 rpm 30 °C. The cells were collected by centrifugation, washed three times with deionized water, and resuspended in one mL of deionized water. 100 µL of the bacterial suspension was added to 20 mL nitrogen-deficient medium (prepared with deionized water and supplemented with 100 mM NH_4Cl as a nitrogen source) with 36 mg/L iron citrate or no iron citrate. After three days of incubation at 200 rpm and 30 °C, all samples were treated with the same method to measure the corresponding OD_{530} value. The content of indolic compounds of each sample was calculated using the Salkowski calibration curve. The nitrogen-deficient medium with deionized water was used as a blank control. Each sample was treated three times.

Antimicrobial assay

The antimicrobial assay was performed according to the recommended guidelines of the National Center for Clinical Laboratory Standards (NCCLS) (*Li et al., 2008*). The bacterial cells of *Escherichia coli* (ATCC1.0090), *Staphylococcus aureus* (ATCC6538), and *Bacillus subtilis* (ATCC6663) were grown in Mueller-Hinton Broth (MHB) medium (5.0 g beef powder, 1.5 g starch, 17.5 g acid hydrolyzed casein, and 1 L H_2O) at 37 °C for 24 h. The fungus (yeast), *Candida albicans* (CGMCC2.2086), was grown in Saurer's Dextrose Broth (SDB) medium (5 g casein trypsin digest, 5 g gastric enzyme digest, 20 g dextrose and 1 L ddH_2O) at 28 °C for 48 h.

The cells of bacteria and yeast cultivated in MHB and SDB media as described above were seeded onto each well of a 96-well clear plate, then the gradient concentrations of test compounds **1-6** were added to each well and mixed with the targeted microbes to reach a final volume of 100 µL. The inoculation concentrations of bacteria and yeast were $0.5-2.5 \times 10^5$ cfu / mL and $0.5-2.5 \times 10^3$ cfu / mL, respectively. The suspension was cultured at 37 °C for 1 day and 28 °C for 2 days, respectively. Gentamicin, ampicillin, sulphate streptomycin, and amphotericin B were used as positive controls. A microplate reader was employed to perform at the OD_{595}. The IC_{50} of compounds **1-6** were plotted, calculated, and obtained. Each antimicrobial assay was tested in triplicate.

Siderophores detection by blue agar CAS assay

Siderophores were detected using a blue agar CAS medium as described by *Schwyn & Neilands (1987)*. The solid CAS medium was composed of one mL 20% sucrose solution, three mL sterilized 10% casamino acid, 100 µL one mmol/L $CaCl_2$, five mL CAS dye solution (a mixture of 0.012 g of chrome azurol S in 10 mL of ddH_2O, two mL one mmol/L $FeCl_3$, and 0.015 g hexadecyltrimethylammonium bromide in eight mL of deionized H_2O), PIPES buffer (pH 6.8–7.0), and 2 g agar powder per 100 mL H_2O.

P. triticisoli BJ-18 was inoculated in 20 mL of liquid LB medium with shaking at 200 rpm at 30 °C for 48 h. one mL of the bacterial solution was centrifuged, washed with sterile deionized water, and then suspended with 200 µL of sterile deionized H_2O. 10 µL of the suspension was inoculated on a CAS plate. The color changed from blue to light orange, indicating the presence of iron carriers.
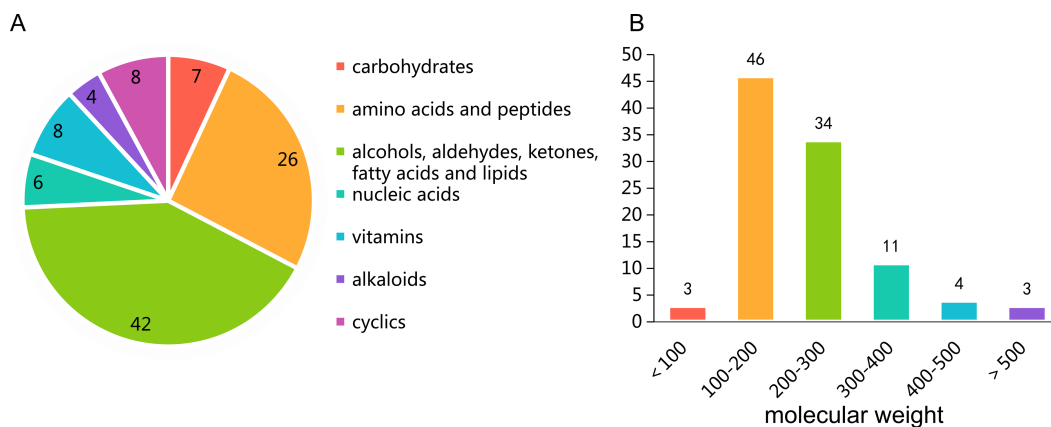
Figure 1 Untargeted metabolomics profiling of *P triticisoli* BJ-18. (A) Number of compounds of different types; (B) Number of compounds in different molecular weight.

RESULTS

Untargeted metabolomics profiling of *P. triticisoli* BJ-18

The untargeted metabolomics profiling of *P. triticisoli* BJ-18 were analyzed by using LC-MS and the data were comparatively analyzed with the databases of mzCloud, ChemSpider and mzVault. A total of 101 compounds were measured, the majority of which were common compounds involved in the basic metabolism (Table S1), including carbohydrates, amino acids, peptides, alcohols, aldehydes, ketones, fatty acids, lipids, nucleic acids, vitamins, alkaloids, cyclics and their respective derivatives (Fig. 1A). Of the 101 compounds, 46 have the molecular weights of 100–200 Da, 34 have the molecular weights of 200–300 Da, 18 have the molecular weights of more than 300 Da and 3 have the molecular weights of less than 100 Da (Fig. 1B).

Notably, N^2-acetyl ornithine, a precursor to fusarinines, is included among these compounds. Also, plant growth regulators such as trehalose 6-phosphate (T6P, resistant to drought and salt stress. *Wingler et al., 2012*; *Prasad et al., 2014*; *Kretzschmar et al., 2015*), betaine (a non-toxic osmotic regulator. (*Cho et al., 2003*; *Tramontano & Jouve, 1997*) and trigonelline (resistant to salt stress. *Minorsky, 2002*; *Tramontano & Jouve, 1997*), and other active molecules such as oxymatrine (a drug used to treat hepatitis B and tumors. *Lu et al., 2003*; *Song et al., 2006*), diosmetin (in food or medicine with anti-oxidant properties, anti-infective, and anti-shock functions *Pallab et al., 2019*), luotonin A (anti-tumor drug. *González-Ruiz et al., 2010*), α-humulene (hippone, sesquiterpene, with anti-inflammatory effect. *Rogerio et al., 2009*), (-)-caryophyllene oxide (anti-tumor and antifungal drug. *Yang et al., 1999*; *Park et al., 2011*), tetrahydrocurcumin (hepatotoxicity prevention drug and natural whitening ingredients. *Pari & Murugan, 2004*; *Trivedi et al., 2017*) were also included among these compounds.
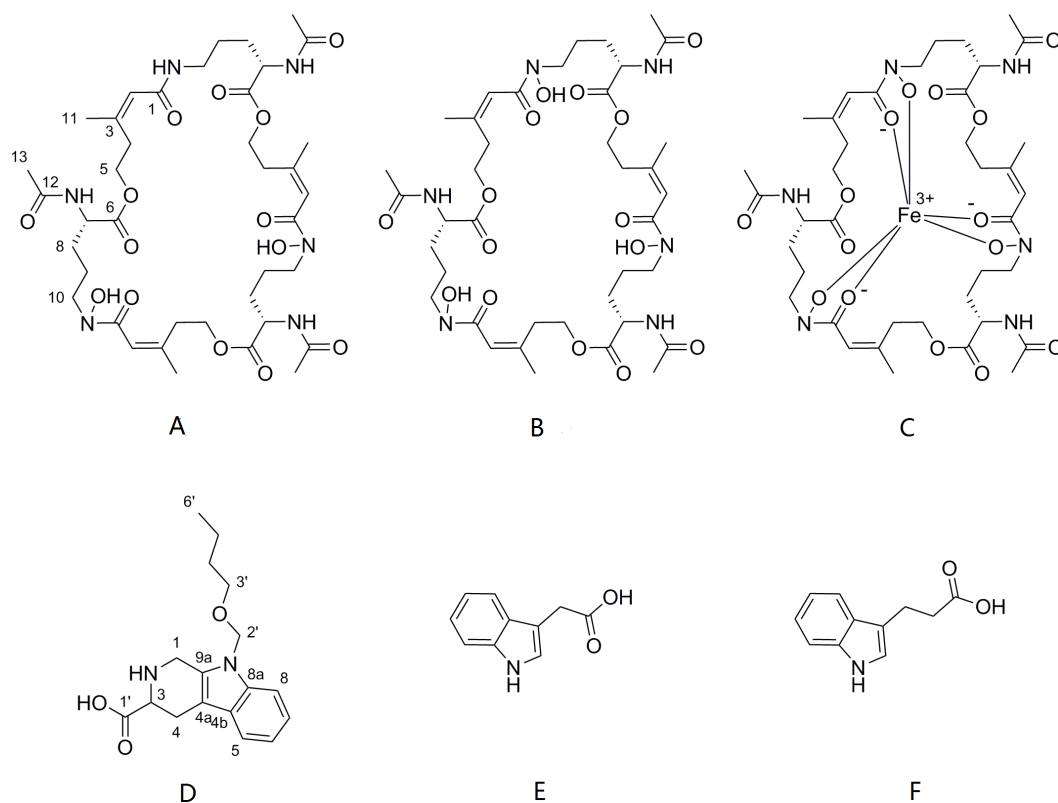
Figure 2 Compounds isolated from *P. triticisoli* BJ-18. Six compounds were isolated from *P. triticisoli* BJ-18, including three classical siderophore fusarinines identified as (A) deshydroxylferritriacetylfusigen, (B) desferritriacetylfusigen and (C) triacetylfusigen, and three indolic acids identified as (D) paenibacillic acid A, (E) 3-indoleacetic acid(IAA), and (F) 3-indolepropionic acid (IPA).

Full-size ⊡ DOI: 10.7717/peerj.9403/fig-2

Structural determination of secondary metabolites from *P. triticisoli* BJ-18

The cells of *P. triticisoli* BJ-18 were fermented and concentrated, and 4 g of EtOAc extracts was obtained. The extracts were separated using a combination of silica gel chromatography, sephadex LH-20, ODS column chromatography, and HPLC. Six compounds (compounds **1**-**6**) were ultimately obtained and were further analyzed using NMR and MS to establish their structures. Further the structure and characters of the six compounds (compounds **1**-**6**) were compared with the corresponding compounds in the literature. Among the six compounds, compounds **1**-**3** were identified as fusarinines that were classical siderophores, while compounds **4**-**6** were identified as indolic acids (Fig. 2). Both compound **1** and **4** have new structures.

Compound **2** was a cyclic tripolymer which has three same monomers (m/z 284.1366) identified as desferritriacetylfusigen (*Anke, 1977*). It was characterized by ^{1}H NMR (500 MHz, DMSO-d_6), δ_H 9.70 (s), 8.21 (d, $J = 7.5$ Hz), 6.32 (s), 4.30–4.03 (m, 3H), 3.33 (s), 2.81 (m), 1.88 (s), 1.85 (s), 1.75–1.39 (m, 4H) (Fig. S1) and by ^{13}C NMR (125 MHz, DMSO-d_6) δ_C 22.7, 23.5, 25.8, 28.5, 32.4, 46.8, 52.3, 63.5, 117.9, 150.1, 167.4, 170.0, 172.6 (Fig. S2). Compound **5** was identified as 3-indoleacetic acid (IAA) (*Gathungu et al., 2014*).

As shown in Fig. S2 , it was characterized by ^{1}H NMR (500 MHz, DMSO-d_6), δ_H 12.14 (s), 10.90 (s), 7.49 (d, $J = 7.9$ Hz), 7.34 (d, $J = 8.1$ Hz), 7.22 (d, $J = 2.3$ Hz), 7.07 (t, $J = 7.6$ Hz), 6.98 (t, $J = 7.4$ Hz), 3.63 (s, 2H). Compound **6** was identified as 3-indolepropionic acid (IPA) (*Rustamova et al., 2019*). As shown in Fig. S4, it was characterized by ^{1}H NMR (500 MHz, acetone-d_6), δ_H 9.97 (s), 7.59 (d, $J = 7.9$ Hz), 7.37 (d, $J = 8.1$ Hz), 7.16 (s), 7.09 (t, $J = 7.5$ Hz), 7.02 (t, $J = 7.5$ Hz), 3.06 (t, $J = 7.7$ Hz), 2.70 (t, $J = 7.7$ Hz).

Compound **1** was a new member of fusarinines (siderophores) and compound **4** was a new member of the indolic acids. Their structures were further determined by extensive spectroscopic experiments. The structure of compound **3** was determined by NMR after iron was removed and it was identified as triacetylfusigen. Overall, the six compounds include three fusarinines (siderophores) and three indolic acids. (Fig. 2).

Compounds **1**, **3**, and **4**, are described in greater detail as follows:

Deshydroxylferritriacetylfusigen (compound **1**) was a yellow powder with a molecular formula of $C_{39}H_{60}N_6O_{14}$ (thirteen degrees of unsaturation) by HRESIMS m/z 837.4242 [M + H]$^+$ (calculated for $C_{39}H_{61}N_6O_{14}$, 837.4246). Its ^{1}H, ^{13}C and HSQC NMR spectroscopic data (Figs. S5–S7) suggested the existence of two methyl groups ($\delta_{C/H}$22.3/1.84 and 25.3/1.87), five methylenes, including one O-methylene ($\delta_{C/H}$63.1/4.17 and 4.12), one double bond ($\delta_{C/H}$117.5/6.31 and δ_C 149.6), three carboxylic carbons (δ_C 166.0, 169.5 and 172.1), one N-methine ($\delta_{C/H}$ 51.8/4.19), one amide N-H proton (δ_H 8.23), and one amide N-OH proton (δ_H9.92). Thirteen carbon signals in the ^{13}C NMR and thirty-nine in the molecular formula indicated that compound **1** was a cyclic tripolymer similar to compound **2**. Comparison of MS-MS spectrum of compound **1** (Fig. S8) and compound **2** (Fig. S9) revealed that unlike compound **2**, two of the three monomers of compound **1** have the same molecular weight as the monomers of compound **2** (m/z 284.1366), and the other was different (m/z 268.1566). The molecular weight of this unique monomer is 16 less than that of others, which is the molecular weight of an oxygen atom. Although the NMR of compound **1** was similar to compound **2**, the integration of N-OH protons in ^{1}H NMR of compound **1** was less than compound **2**. The molecular formula also suggested that there were only two hydroxyls in compound **1** rather than three. The planar structure was confirmed by combining ^{1}H-^{1}H COSY and HMBC (Figs. S10 & S11, Fig. 3). The ROESY spectrum (Fig. S12) showed that CH$_3$-11 had the NOE correlation with the olefinic proton (δ_H6.31) indicating that the double bond was in a Z- configuration. Compound **2** was deduced to come from ornithine (*Schrettl et al., 2007*), and the absolute configuration of compound **1** was determined to be 5S. Our data suggested that compound **1** has a new structure and we proposed the name deshydroxylferritriacetylfusigen for the new number of fusarinines (Table 1).

Compound **3** was a brown powder with a molecular formula of $C_{39}H_{57}N_6O_{15}Fe$ by HRESIMS ([M + H]$^+$ at m/z 906.3316, calculated for $C_{39}H_{58}N_6O_{15}Fe$, 906.3309). Compound **3** had no signal of NMR (Fig. S13) due to its metal-shielding characteristics. A strong complexing agent (*Kodani et al., 2015*) desferri-compound **3** was a yellow powder with a molecular formula of $C_{39}H_{60}N_6O_{15}$ (thirteen degrees of unsaturation) by HRESIMS ([M + H]$^+$ at m/z 853.4203, calculated for $C_{39}H_{60}N_6O_{15}$, 853.4195) obtained following the precipitation and separation of the metal ions by 8-quinolinol. Analysis of its HRESIMS

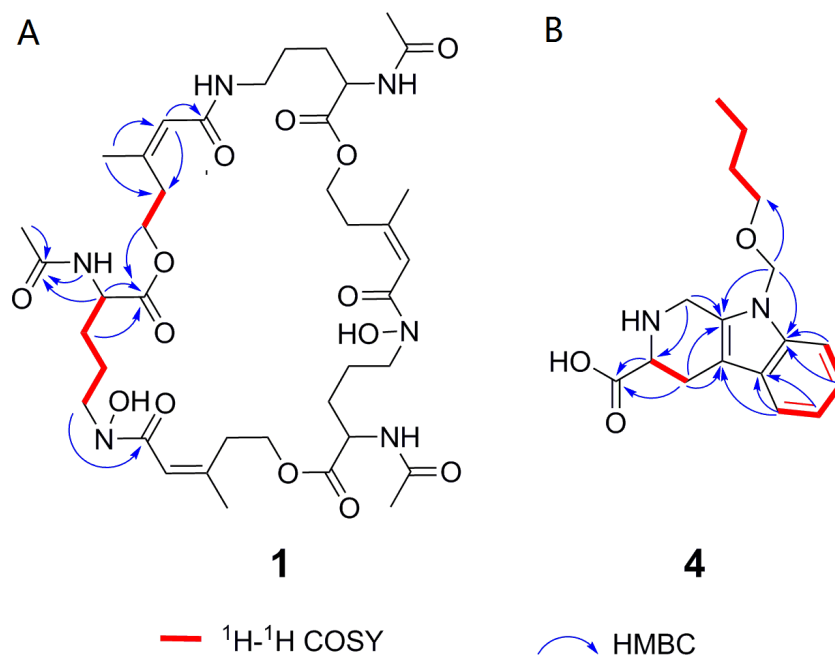**Figure 3 Key ^{1}H-^{1}H COSY and HMBC correlations of compounds 1 and 4.** ^{1}H-1H COSY spectra (DMSO-d_6, 8 MHz); HMBC spectra (DMSO-d_6, 8 MHz).

Full-size 🖻 DOI: 10.7717/peerj.9403/fig-3

and ^{1}H NMR (Fig. S14) data revealed that desferri-compound **3** had the same structure as compound **2**. Compound **3** was determined to be a ferri-complex compound, identified as triacetylfusigen.

Compound **4** was isolated as white amorphous powder with the molecular formula of $C_{17}H_{22}N_2O_3$ (eight degrees of unsaturation) determined by HRESIMS *m/z* 303.1704 $[M + H]^+$ (calculated for $C_{17}H_{23}N_2O_3$ 303.1708). The ^{1}H and ^{13}C NMR combining with HSQC (Figs. S15–S17) revealed one methyl group [$\delta_{C/H}$13.6/0.78 (t, $J = 7.4$Hz)], six methylenes, including two *O*-methylene [$\delta_{C/H}$ 67.1/3.30 (m) and 72.3/5.46 (s)], one ethane [δ_C 56.1/3.63 (dd, $J = 10.3, 5.0$)], eight aromatic/olefinic carbons (δ_C 108.2, 109.8, 118.1, 119.7,121.9, 126.2, 129.4 and 137.2) and one carboxylic carbons (δ_C170.0). These data suggested that compound **4** was similar to lycoperodine-1 (*Yahara et al., 2004*). The ^{1}H–^{1}H COSY data (Fig. S18) revealed four isolated proton spin-systems of C-1-N-C-3-C-4, C-5–C-6, C-7–C-8, and C-3′–C-4′–C-5′–C-6′, respectively. The HMBC spectrum (Fig. S19) showed correlations from H-2′ to C-3′, C-8a and C-9a, from H-1 to C-3 and C-9a, from H-3 and H-4 to C-1, from H-4 to C-9a and C-4a, from H-5 to C-5a and C-4a, and from H-7 and H-8 to C-8a. The planar structure of compound **4** was established by linking these fragments (Fig. 3 & Table 2). The ECD calculation method (*Ma et al., 2014*) was used to determine the absolute configurations. The structure of compound **4** was simplified into two stereoisomers **4a** (3*S*) and **4b** (3*R*). The calculated ECD curve of compound **4a** correlated with the experimental CD spectrum of **4** (Fig. 4). The absolute configuration of compound **4** was established as 3*S* using the time-dependent density functional theory
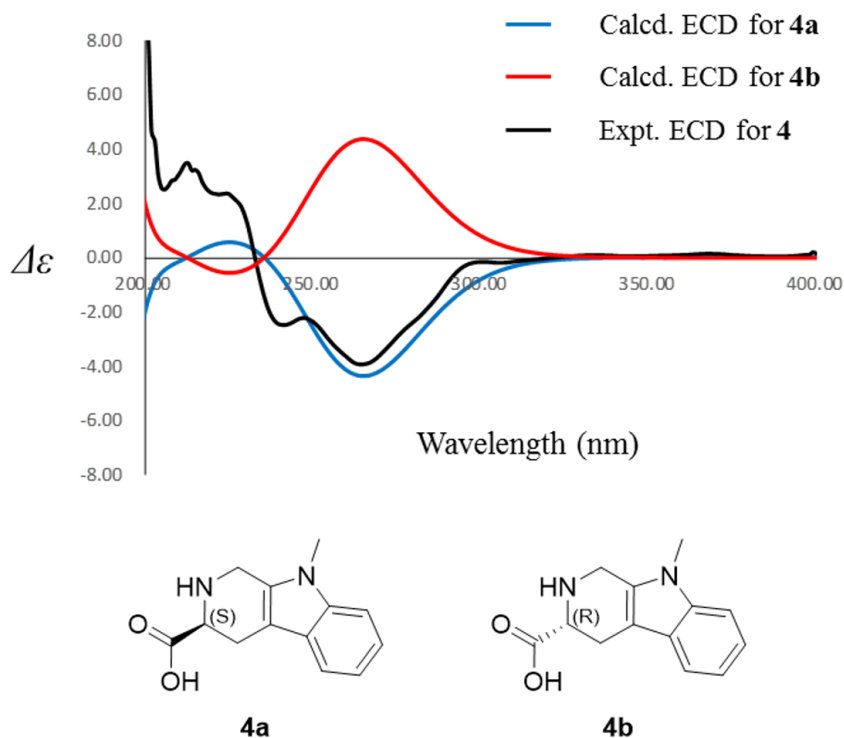
Figure 4 Experimental ECD spectra of 4 and its calculated ECD spectra of related simplified possible stereoisomers 4a and 4b. Experimental ECD spectra of 4 was recorded in methanol. Systematic conformation analysis of 4a was conducted with CONFLEX using the MMFF94 molecular mechanics force field. Optimization with DFT calculation at the B3LYP/6-31G(d) level in MeOH by the Gaussian09 program afforded the MMFF minima. At the B3LYP/6-31G(d) level, the exciting states were calculated using time-dependent density-functional theory (TDDFT) methodology for 4a. The overall ECD spectra were then produced based on Boltzmann weighting of each conformer.

Full-size 🖼 DOI: 10.7717/peerj.9403/fig-4

(TDDFT) at the B3LYP/6-311G (d,p) level (Fig. S20). Compound **4** was the derivative of IPA (here named paenibacillic acid A).

Effects of indolic acids compounds on plant growth promotion

The effects of indolic acids compounds on growth of *Arabidopsis thaliana* var. Columbia were investigated. Paenibacillic acid A, IAA, and IPA were shown to promote the growth of plant shoots and roots (Fig. 5) as well as the dry weight of the plants (Fig. 6). The growth-promoting ability increased as the concentration of paenibacillic acid A, IAA, and IPA increased until their highest growth-promoting ability was attained, and then their plant growth-promoting ability decreased with increasing concentration. The significant efficiencies of plant-growth promotion were obtained when the concentrations of paenibacillic acid A, IAA and IPA were at 100 nM, 250 nM and 50 nM, respectively, suggesting that IPA has the strongest ability of plant growth promotion among the three indolic acids compounds.

We further determined the content of indolic compounds produced by *P. triticisoli* BJ-18 when it was measured in the nitrogen-deficient medium with and without iron.
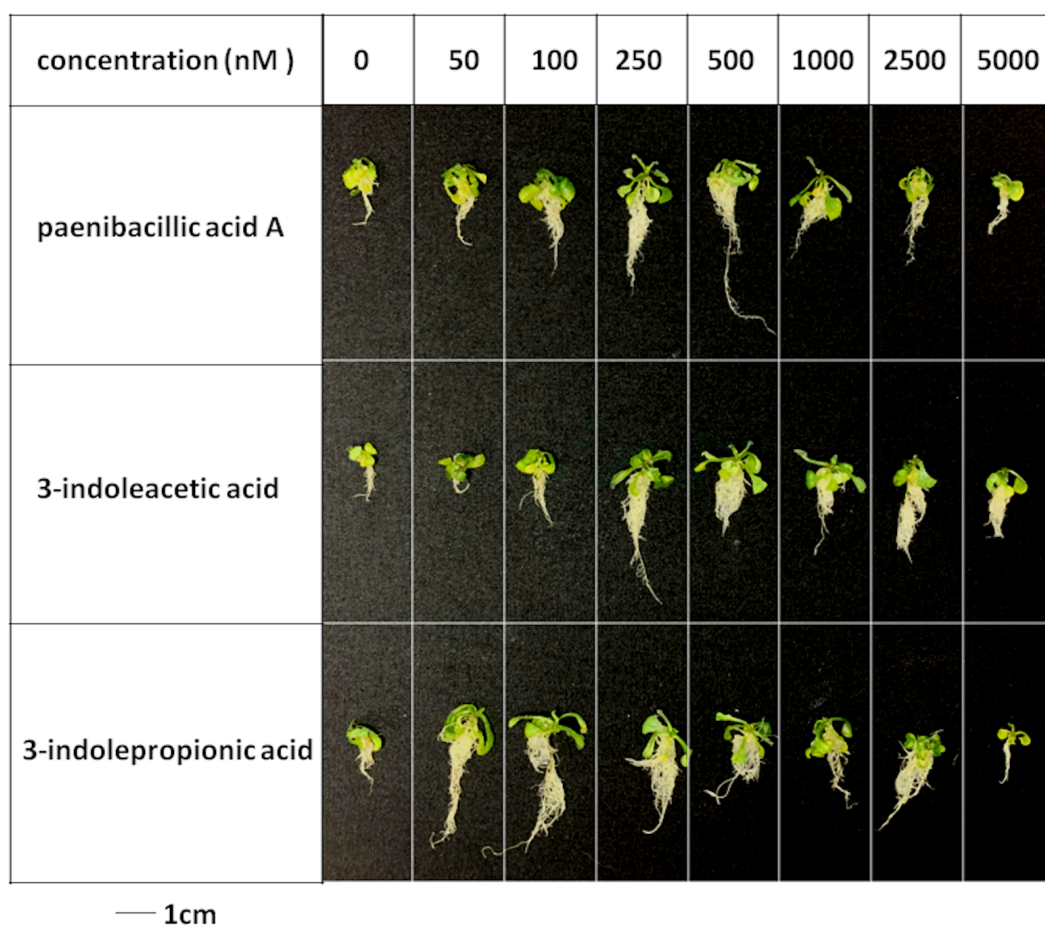
Figure 5 **Plant growth-promoting capacity of indolic compounds on *Arabidopsis thaliana*.** Seeds of *Arabidopsis thaliana* var. Columbia were used as plant material, and were incubated at 25 ± 2 °C under cool fluorescent light (2000 lux 16 h/day photoperiod) for 14 days.

Full-size ◩ DOI: 10.7717/peerj.9403/fig-5

The results showed that *P. triticisoli* BJ-18 produced 37.03 ± 1.21 µg/mL of the indolic compounds in a medium with an iron ion concentration of 4.409×10^{-4} mM and 13.457 ± 0.78 µg/mL of the indolic compounds in a medium without iron, suggesting that the content of indolic compounds in *P. triticisoli* BJ-18 is positively related to the iron in the environment.

Antimicrobial activity

The antimicrobial properties of siderophores and indolic acids were assayed against the indicator strains (bacteria *E. coli*, *S. aureus* and *B. subtilis,* and yeast *C. albicans*) (Table 3). Both compounds **1** and **2** that are siderophores showed antimicrobial activity against *E. coli*, *S. aureus* and *B. subtilis*, but did not show obvious inhibitory activity against yeast *C. albicans*.

Gentamicin, ampicillin, streptomycin sulfate and amphotericin B were used as positive controls against *E. coli*, *S. aureus*, *B. subtilis* and *C. albicans*, respectively. The compounds
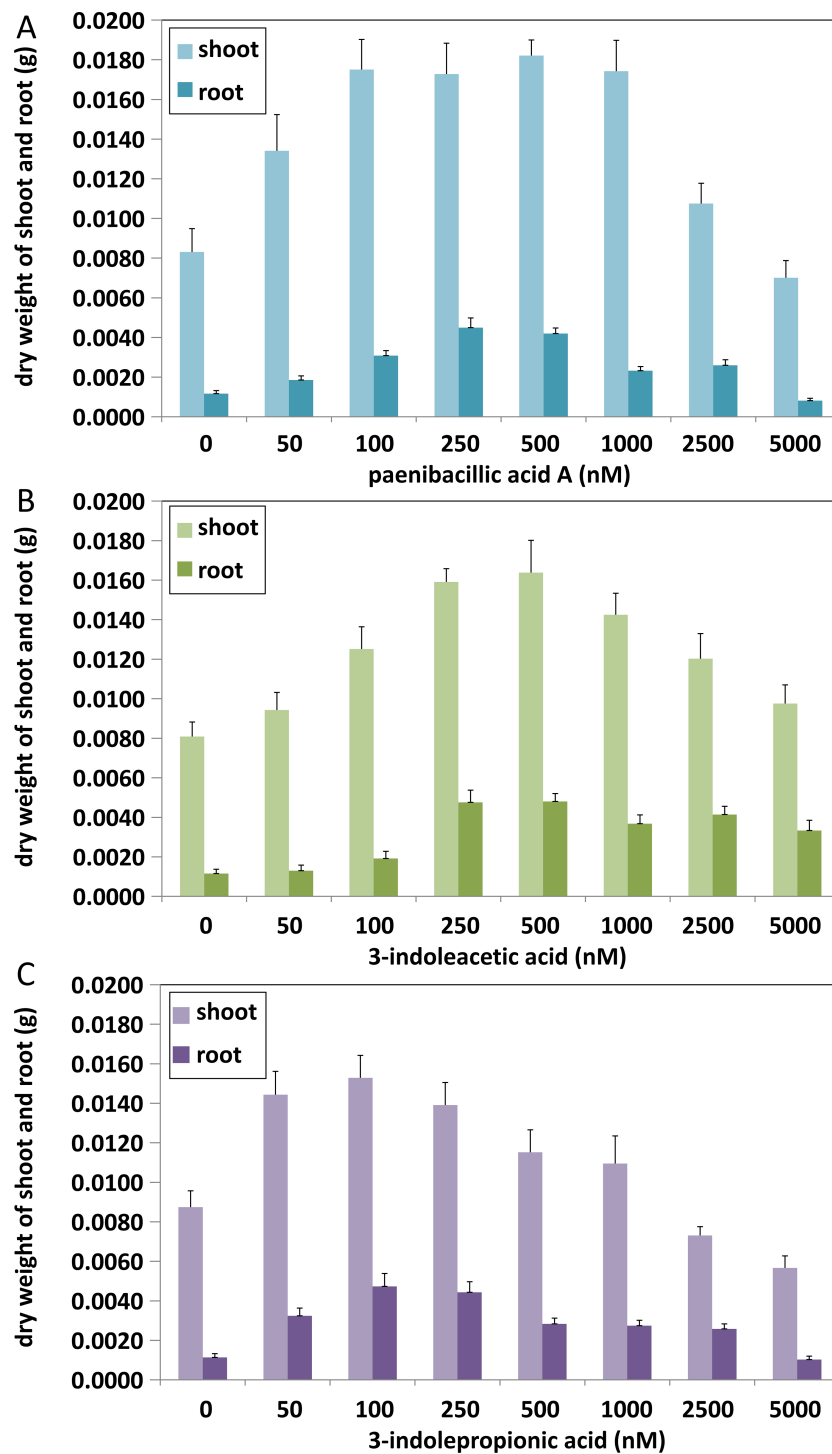
Figure 6 **Comparison of plant growth-promoting ability of indolic compounds.** At least ten *Arabidopsis* strains were cultured in each group of treatments (A, paenibacillic acid A (nM); B, 3-indoleacetic acid (nM); C,3-indolepropionic acid (nM)). The cultures were incubated at 25 ± 2 °C under cool fluorescent light (2000 lux 16 h/day photoperiod) for 14 days.

Table 3 **Antimicrobial activity of compounds 1-6.** Gentamicin, ampicillin, streptomycin sulfate and amphotericin B were used as positive controls against *E. coli*, *S. aureus*, *B. subtilis* and *C. albicans*, respectively. The compounds were tested at concentrations of 5 μm , 10 μm and 20 μm. The IC50 was calculated using the Spearman-Karbers method. The horizontal line "−" indicated that the compound had no antibacterial activity against the indicator strain.

IC$_{50}$ (μM)	*E. coli*	*S. aureus*	*B. subtilis*	*C. albicans*
compound **1**	6.8	5.2	8.8	–
compound **2**	4.7	4.3	6.4	–
compound **3**	–	–	–	–
compound **4**	–	7.4	–	–
compound **5**	–	–	–	–
compound **6**	–	–	–	–
Pos.	1.9	2.1	2.3	2.2

were tested at concentrations of 5 μM, 10 μM and 20 μM. The IC$_{50}$ was calculated using the Spearman-Karber's method.

Siderophore detection by blue agar CAS assay

Siderophore production by *P. triticisoli* BJ-18 was determined by blue agar CAS assay as described in materials and methods. A yellow ring appeared around each colony after seven days of *P. triticisoli* BJ-18 growth on a blue agar plate, indicating that *P. triticisoli* BJ-18 had the ability to secrete siderophores and transfer iron from the environment to the bacterial cells (Fig. S21). The data are consistent with the above results that compounds **1**-**3** are siderophores.

DISCUSSION

P. triticisoli BJ-18, a N$_2$-fixing bacterium, significantly promoted plant growth, but the secondary metabolites produced by this bacterium have never been characterized. In this study, 101 known compounds of *P. triticisoli* BJ-18 were measured by untargeted metabolomics profiling. These compounds include N^2-acetyl ornithine, which is the precursor of fusarinines (siderophores). There are 7 types of siderophores: fusarinines, rhodotorulic acids, ferrichromes, ferrioxamines, aerobactins, enterobactins, and mycobactins (*Hossain et al., 1980*). Fusarinines are synthesized by aminoacyl bonds, making them different from other types of siderophores that are polymerized using peptide linkages. Fusigen, a cyclic trimester of fusarinine, was identified by *Diekmann & Zähner (1967)* and was considered to be the iron ionophore for *Fusar* ium *roseum* (*Sayer & Emery, 1968*). Studies have shown triacetylfusigen, which has three acetyl group in place of the H atoms of the amino, was isolated from *Aspergillus fumigates* (*Diekmann & Krezdorn, 1975*) *and Aspergillus nidulans* (*Charlang et al., 1981*), while desferritriacetylfusigen was found in *Aspergillus deflectus* (*Anke, 1977*) and *Emericella* sp. (*Cruz et al., 2012*). These siderophores were isolated from fungi but bacterial fusarinines have never been identified before our study. Here, three fusarinines were isolated from *P. triticisoli* BJ-18 and identified as deshydroxylferritriacetylfusigen, desferritriacetylfusigen, and triacetylfusigen, of which deshydroxylferritriacetylfusigen was a new structure of

fusarinine. Here is the first study to report the bacterial fusarinine. Ornithine is the only amino acid of fusarinine (*Charlang et al., 1982*). The Kyoto Encyclopedia of Genes and Genomes (KEGG, https://www.kegg.jp/) shows that fusarinine can be synthesized by some specific ornithylesterases including fusarinine-C ornithineesterase, ornithine esterase and 5-N-acyl-L-ornithine-ester hydrolase. Studies on fusarinine in fungi have shown that the specific ornithylesterases promote cellular iron-exchange by hydrolysis of the ester bonds of the ferric ionophores (*Emery, 1976*).

Indolic compounds are natural auxins in plants and rhizosphere microorganisms and can promote the formation of shoot tips, buds, and roots. The auxins commonly used in agriculture are IAA, indolebutyric acid, 2,4-dichlorophenoxyacetic acid and naphthylacetic acid. Three indolic acids identified as paenibacillic acid A, IAA, and IPA were isolated from *P. triticisoli* BJ-18, of which paenibacillic acid A was a new structure. The results of the plant growth promoting capacity assay showed that the three compounds can promote the growth of the shoots and roots of *A. thaliana* and can increase the dry weight of the plant. The effect of paenibacillic acid A on *A. thaliana* is similar to that of IAA. IPA was the best promoter of plant growth among the three indolic compounds. Indolic compounds such as indole, skatole, and indirubin were concurrently identified by untargeted metabolomics profiling. Our results showed that *P. triticisoli* BJ-18 can promote plant growth by synthesizing plant growth hormones, including indolic acids.

Indolic compounds were usually synthesized in two pathways, either by iron (III) complexed by the ligand of indolic compounds or by the reduction of the soluble iron (II) complex. These parallel reactions cannot proceed without iron (*Gazaryan et al., 1996*;*Kovács et al., 2008*; *Xie et al., 2016*). Indolic acid assays showed that the content of indolic compounds of *P. triticisoli* BJ-18 was related to the presence or absence of iron ions. The content of indolic compounds of *P. triticisoli* BJ-18 can reach 37.03 ± 1.21 μg/mL in the medium with an iron ion concentration of 4.409×10^{-4} mM, while the content is 13.457 ± 0.78 μg/mL in the iron-free environment, indicating the importance of iron for the synthesis of indolic compounds.

Phytopathogens must sequester iron to develop and sustain infections (*Ratledge & Dover, 2000*). Competing for iron is a mechanism taken by PGPR to inhibit the growth of phytopathogens in the soil (*Chet et al., 1990*). The six compounds were evaluated for their activities against a panel of microbes. Results showed that desferritriacetylfusigen and deshydroxylferritriacetylfusigen were antimicrobial against *E. coli*, *S. aureus,* and *B. subtilis.* Triacetylfusigen showed no antibiosis activity against any targeted microorganism due to its complexion with iron.

Plant growth regulators such as betaine and trigonelline, and other active molecules such as luotonin A, aphidicolin, oxymatrine, diosmetin, pilocarpine and tetrahydrocurcumin were also identified by untargeted metabolomics profiling. Besides, deshydroxylferritriacetylfusigen had weak cytotoxic activity against AsPC-1 with IC_{50} value of 81.2 ± 3.9 μM (File S1), indicating that siderophores may have potential as a new therapy for human cancers (*Kalinowski & Richardson, 2005*; *Ji, Juárez-Hernández & Miller, 2012*). The chemical composition and application of *P. triticisoli* BJ-18 is far more complicated and promising.
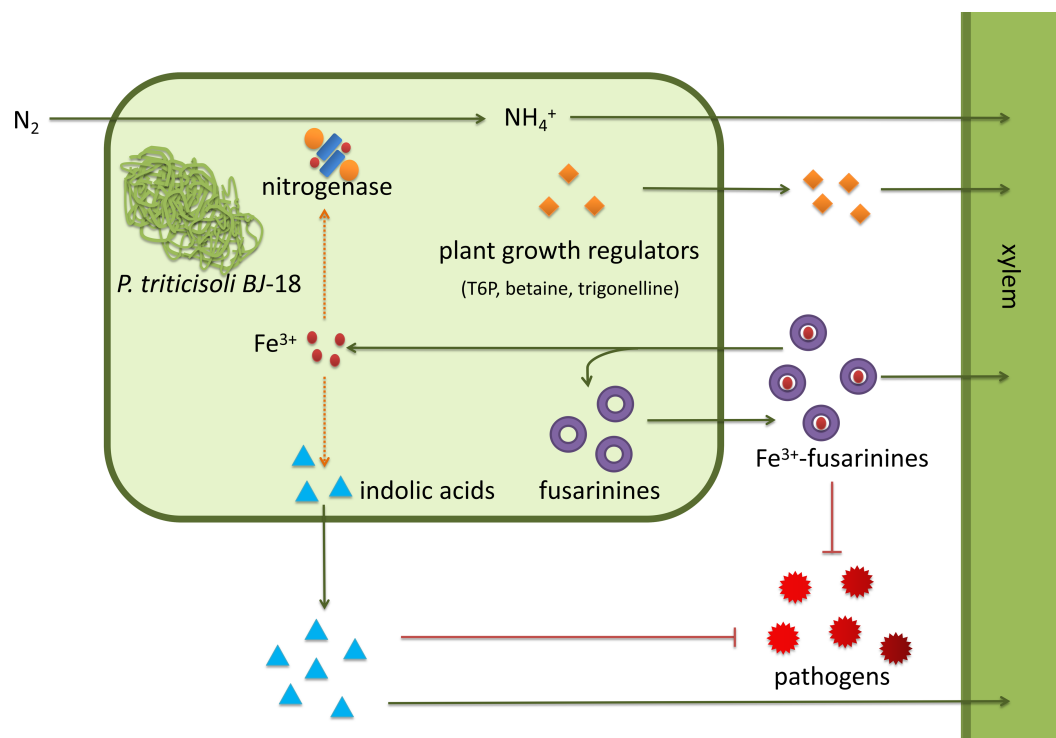
Figure 7 *P. triticisoli* **BJ-18 promotes plant growth by several mechanisms.** The orange squares represent plant growth regulators such as T6P, betaine and trigonelline. The purple ring represents fusarinines and the red dot represents iron atoms. The blue triangle indicates indole acids. Red radial circles represent plant pathogens. Six-component structure representing nitrogenase.

Full-size ⊡ DOI: 10.7717/peerj.9403/fig-7

    P. triticisoli BJ-18 has been shown to promote plant growth using several mechanisms (Fig. 7). *P. triticisoli* BJ-18 provides a nitrogen source for plant growth by N_2-fixation, produces indolic acids to promote plant growth, generates siderophores to capture iron atoms to synthesize nitrogenase and indolic acids, and synthesizes plant growth regulators such as T6P, betaine and trigonelline, and secretes fusarinines and paenibacillic acid A to resist phytopathogens.

    Our results provide chemical evidence for the use of *P. triticisoli* BJ-18 as a PGPR biofertilizer in agriculture. The discovery of the many compounds identified in our study shows the agricultural and medical value of *P. triticisoli* BJ-18. The metabolic regulation of fusarinines and other bioactive compounds requires further study.

CONCLUSIONS

In this study, six compounds were isolated and characterized from *P. triticisoli* BJ-18, a N_2-fixer. The six compounds included three classical siderophore fusarinines identified as deshydroxylferritriacetylfusigen, desferritriacetylfusigen, and triacetylfusigen, and three indolic acids identified as paenibacillic acid A, 3-indoleacetic acid (IAA), and 3-indolepropionic acid (IPA). Both deshydroxylferritriacetylfusigen and paenibacillic acid A have new structures. Fusarinines, which normally occur in fungi, were isolated from

bacteria for the first time in this study. Both siderophores (compounds **1** and **2**) showed antimicrobial activity against *E. coli*, *S. aureus* and *B. subtilis*, but did not show obvious inhibitory activity against yeast *Candida albicans*. Whereas triacetylfusigen (compound **3**) showed no antibiosis activity against these test microorganisms. Paenibacillic acid A, IAA, and IPA were shown to promote the growth of plant shoots and roots, and paenibacillic acid A also showed antimicrobial activity against *S. aureus*. Our study demonstrated that siderophores and indolic acids may play an important role in plant growth promotion by *P. triticisoli* BJ-18.

ADDITIONAL INFORMATION AND DECLARATIONS

Competing Interests

The authors declare there are no competing interests.

Author Contributions

- Yunzhi Zhang conceived and designed the experiments, performed the experiments, analyzed the data, prepared figures and/or tables, authored or reviewed drafts of the paper, and approved the final draft.
- Jinwei Ren and Wenzhao Wang performed the experiments, prepared figures and/or tables, and approved the final draft.
- Baosong Chen analyzed the data, prepared figures and/or tables, and approved the final draft.
- Erwei Li conceived and designed the experiments, performed the experiments, authored or reviewed drafts of the paper, and approved the final draft.
- Sanfeng Chen conceived and designed the experiments, authored or reviewed drafts of the paper, and approved the final draft.

Data Availability

The following information was supplied regarding data availability:
Raw data is available at Figshare: Zhang, Yunzhi (2020): RAW-YZ peerJ.rar. figshare. Dataset. https://doi.org/10.6084/m9.figshare.11996661.v1.

Supplemental Information

Supplemental information for this article can be found online at http://dx.doi.org/10.7717/peerj.9403#supplemental-information.

REFERENCES

Aeron A, Maheshwari DK, Meena VS. 2020. Endophytic bacteria promote growth of the medicinal legume *Clitoria ternatea* L. by chemotactic activity. *Archives of Microbiology* **202**:1049–1058 DOI 10.1007/s00203-020-01815-0.

Anke H. 1977. Metabolic products of microorganisms. Desferritriacetylfusigen, an antibiotic from *Aspergillus deflectus*. *Journal of Antibiotics* **30(2)**:125–128 DOI 10.7164/antibiotics.30.125.

Arora NK, Kang SC, Maheshwari DK. 2001. Isolation of siderophore-producing strains of *Rhizobium meliloti* and their biocontrol potential against *Macrophomina phaseolina* that causes charcoal rot of groundnut. *Current Science* **81(6)**:673–677.

Backer R, Rokem JS, Ilangumaran G, Lamont J, Praslickova D, Ricci E, Subramanian S, Smith DL. 2018. Plant growth-promoting rhizobacteria: context, mechanisms of action, and roadmap to commercialization of biostimulants for sustainable agriculture. *Frontiers in Plant Sciencei* **9**:1473 DOI 10.3389/fpls.2018.01473.

Banerjee MR, Yesmin L, Vessey JK. 2006. Plant-growth-promoting rhizobacteria as biofertilizers and biopesticides. In: *Handbook of microbial biofertilizers.* Binghamton: Food Products Press, 137–183.

Beck HC, Hansen AM, Lauritsen FR. 2003. Novel pyrazine metabolites found in polymyxin biosynthesis by *Paenibacillus polymyxa*. *FEMS Microbiology Letters* **220(1)**:67–73 DOI 10.1016/S0378-1097(03)00054-5.

Beneduzi A, Peres D, Costa PBD, Zanettini MHB, Passaglia LMP. 2008. Genetic and phenotypic diversity of plant-growth-promoting bacilli isolated from wheat fields in southern Brazil. *Research in Microbiology* **159(4)**:0–250.

Braun V, Braun M. 2002. Iron transport and signaling in *Escherichia coli*. *FEBS Letters* **529(1)**:78–85 DOI 10.1016/S0014-5793(02)03185-X.

Castellano HA, Pérez TV, Bedmar EJ, Santillana N. 2018. Purple corn-associated rhizobacteria with potential for plant growth promotion. *Journal of Applied Microbiology* **124(5)**:1254–1264 DOI 10.1111/jam.13708.

Charlang G, Horowitz RM, Lowy PH, Ng B, Poling SM, Horowitz NH. 1982. Extracellular siderophores of rapidly growing *Aspergillus nidulans* and *Penicillium chrysogenum*. *Journal of Bacteriology* **150(2)**:785–787 DOI 10.1128/JB.150.2.785-787.1982.

Charlang G, Ng B, Horowitz NH, Horowitz RM. 1981. Cellular and extracellular siderophores of *Aspergillus nidulans* and *Penicillium chrysogenum*. *Molecular and Cellular Biology* **1(2)**:94–100 DOI 10.1128/MCB.1.2.94.

Chen L, Dick WA, Streeter JG. 2000. Production of aerobactin by microorganisms from a compost enrichment culture and soybean utilization. *Journal of Plant Nutrition* **23(11–12)**:2047–2060 DOI 10.1080/01904160009382164.

Chen X, Cao F, Li Z, Wu T, Ran L. 2006. Role of siderophore, DAPG and PCA in suppression of conidia in *Cryphonectria parasitica*. *Hebei Journal of Forestry and Orchard Reaserch* **21(4)**:404–408.

Chet I, Ordentlich A, Shapira R, Oppenheim AB. 1990. Mechanisms of biocontrol of soil-borne plant-pathogens by rhizobacteria. *Plant Soil* **129**(**1**):85–92 DOI 10.1007/BF00011694.

Cho Y, Njiti VN, Chen X, Lightfoot DA, Wood AJ. 2003. Trigonelline concentration in field-grown soybean in response to irrigation. *Biologia Plantarum* **46**(**3**):405–410 DOI 10.1023/A:1024390522259.

Costacurta A, Vanderleyden J. 1995. Synthesis of phytohormones by plant-associated bacteria. *Critical Reviews in Microbiology* **21**(**1**):1–18 DOI 10.3109/10408419509113531.

Cruz M, Martín J, González-Menéndez V, Pérez-Victoria I, Moreno C, Tormo JR, Aouad NEl, Guarro J, Vicente F, Reyes F, Bills GF. 2012. Chemical and physical modulation of antibiotic activity in *Emericell* a species. *Chemistry and Biodiversity* **9**(**6**):1095–113 DOI 10.1002/cbdv.201100362.

Diekmann H, Krezdorn E. 1975. Metabolic products of microorganisms, ferricrocin, triacetylfusigen and other sideromines from fungi of the genus *Aspergillus*, group *Fumigatus*. *Archives of Microbiology* **106**(**3**):191–194 DOI 10.1007/BF00446522.

Diekmann H, Zähner H. 1967. Constitution and catabolism of fusigen to delta-2-anhydromevalonic acid lactone. *European Journal of Biochemistry* **3**(**2**):213–215 DOI 10.1111/j.1432-1033.1967.tb19518.x.

Duijff BJ, Meijer JW, Bakker PAHM, Schippers B. 1993. Siderophore-mediated competition for iron and induced resistance in the suppression of fusarium wilt of carnation by fluorescent *Pseudomonas* spp. *Netherlands Journal of Plant Pathology* **99**(**5-6**):277–289 DOI 10.1007/BF01974309.

Emery T. 1976. Fungal ornithine esterases: relationship to iron transport. *Biochemistry* **15**(**13**):2723–2728 DOI 10.1021/bi00658a002.

Franco-Sierra ND, Posada LF, Santa-María G, Romero-Tabarez M, Villegas-Escobar V, Álvarez JC. 2020. *Bacillus subtilis* EA-CB0575 genome reveals clues for plant growth promotion and potential for sustainable agriculture. *Functional and Integrative Genomics* **20**:575–589.

Galloway JN, Townsend AR, Erisman JW, Bekunda M, Cai Z, Freney JR, Martinelli LA, Seitzinger SP, Sutton MA. 2008. Transformation of the nitrogen cycle: recent trends, questions, and potential solutions. *Science* **320**:889–892 DOI 10.1126/science.1136674.

Gathungu RM, Bird SS, Sheldon DP, Kautz R, Vouros P, Matson WR, Kristal P. 2014. Identification of metabolites from liquid chromatography–coulometric array detection profiling: gas chromatography–mass spectrometry and refractionation provide essential information orthogonal to LC–MS/microNMR. *Analytical Biochemistry* **454**(**2**):23–32 DOI 10.1016/j.ab.2014.01.020.

Gazaryan IG, Lagrimini LM, Ashby GA, Thorneley RN. 1996. Mechanism of indole-3-acetic acid oxidation by plant peroxidases: anaerobic stopped-flow spectrophotometric studies on horseradish and tobacco peroxidases. *Biochemical Journal* **313**(**3**):841–847 DOI 10.1042/bj3130841.

Glick BR. 2012. Plant growth-promoting bacteria: mechanisms and applications. *Scientifica* **2012**:1–15.

Glickmann E, Dessaux Y. 1995. A critical examination of the specificity of the salkowski reagent for indolic compounds produced by phytopathogenic bacteria. *Applied and Environmental Microbiology* **61(2)**:793–796 DOI 10.1128/AEM.61.2.793-796.1995.

González-Ruiz V, Mussardo P, Corda E, Girotti S, Martín MA. 2010. Liquid chromatographic analysis of the anticancer alkaloid luotonin a and some new derivatives in human serum samples. *Journal of Separation Science* **33(14)**:2086–2093 DOI 10.1002/jssc.201000175.

Guerinot ML. 1994. Microbial iron transport. *Annual Review of Microbiology* **48(1)**:743–772 DOI 10.1146/annurev.mi.48.100194.003523.

Gupta V, Roper MM, Roget DK. 2006. Potential for non-symbiotic N_2 fixation in different agroecological zones of southern Australia. *Australian Journal of Soil Research* **44**:343–354 DOI 10.1071/SR05122.

Haas D, Defago G. 2005. Biological control of soil-borne pathogens by *Fluorescent pseudomonads*. *Nature Reviews Microbiology* **3(4)**:307–319 DOI 10.1038/nrmicro1129.

Hossain MB, Eng-Wilmot DL, Loghry RA, Dick VDH. 1980. Circular dichroism, crystal structure, and absolute configuration of the siderophore ferric N, N′, N″-triacetylfusarinine, $FeC_{39}H_{57}N_6O_{15}$. *Journal of the American Chemical Society* **102(18)**:5766–5773 DOI 10.1021/ja00538a012.

Hutchins DA, Witter AE, Butler A, Luther GW. 1999. Competition among marine phytoplankton for diferent chelated iron species. *Nature* **400(6747)**:858–861 DOI 10.1038/23680.

Ji C, Juárez-Hernández RE, Miller MJ. 2012. Exploiting bacterial iron acquisition: siderophore conjugates. *Future Medicinal Chemistry* **4(3)**:297–313 DOI 10.4155/fmc.11.191.

Kalinowski DS, Richardson DR. 2005. The evolution of iron chelators for the treatment of iron overload disease and cancer. *Pharmacological Reviews* **57(4)**:547–583 DOI 10.1124/pr.57.4.2.

Kazamia E, Sutak R, Paz-Yepes J, Dorrell RG, Vieira FRJ, Mach J, Morrissey J, Leon S, Lam F, Pelletier E, Camadro JM, Bowler C, Lesuisse E. 2018. Endocytosis-mediated siderophore uptake as a strategy for Fe acquisition in diatoms. *Science Advances* **4**:eaar4536 DOI 10.1126/sciadv.aar4536.

Katzy EI, Iosipenko AD, Egorenkov DA, Zhuravleva EA, Panasenko VI, Ignatov VV. 1990. Involvement of *Azopirillum brasilense* plasmid DNA in the productio of indole acetic acid. *FEMS Microbiology Letters* **72(1)**:1–4 DOI 10.1111/j.1574-6968.1990.tb03851.x.

Khan MS, Gao J, Chen X, Zhang M, Yang F, Du Y, Moe TS, Munir I, Xue J, Zhang X. 2020. Isolation and characterization of plant growth-promoting endophytic bacteria *Paenibacillus polymyxa* SK1 from Lilium lancifolium. *Biomed Research International* **2020**:8650957 DOI 10.1155/2020/8650957.

Kodani S, Komaki P, Suzuki M, Kobayakawa F, Hemmi H. 2015. Structure determination of a siderophore peucechelin from *Streptomyces peucetius*. *Biometals* **28(5)**:791–801 DOI 10.1007/s10534-015-9866-4.

Kovács K, Sharma VK, Kamnev AA, Kuzmann E, Homonnay Z, Vértes A. 2008. Water and time dependent interaction of iron(III). *Structural Chemistry* **19(1)**:109–114 DOI 10.1007/s11224-007-9259-6.

Kretzschmar T, Pelayo MAF, Trijatmiko KR, Gabunada LFM, Alam R, Jimenez R, Mendioro MS, Slamet-Loedin IH, Sreenivasulu N, Bailey-Serres J, Ismail AM, Mackill DJ, Septiningsih EM. 2015. A trehalose-6-phosphate phosphatase enhances anaerobic germination tolerance in rice. *Nature Plants* **1(9)**:15124 DOI 10.1038/nplants.2015.124.

Kumari M, Thakur IS. 2018. Biochemical and proteomic characterization of *Paenibacillus* sp. ISTP10 for its role in plant growth promotion and in rhizostabilization of cadmium. *Bioresource Technology Reports* **55(5)**:694–699.

Lambrecht M, Okon Y, Broek AV, Vanderleyden J. 2000. Indole-3-acetic acid: a reciprocal signalling molecule in bacteria-plant interactions. *Trends in Microbiology* **8(7)**:298–300 DOI 10.1016/S0966-842X(00)01732-7.

Lebuhn M, Heulin T, Hartmann A. 1997. Production of auxin and other indolic and phenolic compounds by *Paenibacillus polymyxa* strains isolated from different proximity to plant roots. *FEMS Microbiology Ecology* **22(4)**:325–334 DOI 10.1111/j.1574-6941.1997.tb00384.x.

Li E, Jiang L, Guo L, Zhang H, Che Y. 2008. Pestalachlorides A-C, antifungal metabolites from the plant endophytic fungus *Pestalotiopsis adusta*. *Bioorganic and Medicinal Chemistry* **16(17)**:7894–7899 DOI 10.1016/j.bmc.2008.07.075.

Li YB, Li YL, Zhang H, Wang M, Chen S. 2019. Diazotrophic *Paenibacillus beijingensis* BJ-18 provides nitrogen for plant and promotes plant growth, nitrogen uptake and metabolism. *Frontiers in Microbiology* **10**:1119.

Liu L, Bao L, Wang L, Ma K, Han J, Yang Y, Liu R, Ren J, Yin W, Wang W, Liu HW. 2018a. Asperorydines A-M: prenylated tryptophan-derived alkaloids with neurotrophic effects from *Aspergillus oryzae*. *The Journal of Organic Chemistry* **83(2)**:812–822 DOI 10.1021/acs.joc.7b02802.

Liu H, Carvalhais LC, Crawford M, Singh E, Dennis PG, Pieterse CMJ, Schenk PM. 2017. Inner Plant values: diversity, colonization and benefits from endophytic bacteria. *Frontiers in Microbiology* **8**:1–17.

Liu Y, Wang Z, Bilal M, Hu H, Wang W, Huang X, Peng H, Zhang X. 2018b. Enhanced fluorescent siderophore biosynthesis and loss of phenazine-1-carboxamide in phenotypic variant of *Pseudomonas chlororaphis* HT66. *Frontiers in Microbiology* **9**:759 DOI 10.3389/fmicb.2018.00759.

Lu LG, Zeng MD, Mao YM, Li JQ, Wan MB, Li CZ, Chen CW, Fu QC, Wang JY, She WM, Cai XJ, Ye J, Zhou XQ, Wang H, Wu SM, Tang MF, Zhu JS, Chen WX, Zhang HQ. 2003. Oxymatrine therapy for chronic hepatitis B: a randomized double-blind and placebo-controlled multi-center trial. *World Journal of Gastroenterology* **9(11)**:2480–2483 DOI 10.3748/wjg.v9.i11.2480.

Lucy M, Reed E, Glick BR. 2004. Applications of free living plant growth-promoting rhizobacteria. *Antonie van Leeuwenhoek* **86**(**1**):1–25 DOI 10.1023/B:ANTO.0000024903.10757.6e.

Ma K, Ren J, Han J, Bao L, Liu H. 2014. Ganoboninketals A-C, antiplasmodial 3, 4-seco-27-norlanostane triterpenes from *Ganoderma boninense* Pat. *Journal of Natural Products* **77**(**8**):1847–1852 DOI 10.1021/np5002863.

Mao X, Tang L, Tan T, Wan Y. 2014. Determination of plant growth regulators in pears by microwave-assisted extraction and liquid chromatography with electrospray ionization mass spectrometry. *Journal of Separation Science* **37**(**11**):1352–1358 DOI 10.1002/jssc.201301291.

Menéndez E, Pérez-Yépez J, Hernández M, Rodríguez-Pérez A, Velázquez E, León-Barrios M. 2020. Plant growth promotion abilities of phylogenetically diverse *Mesorhizobium* strains: effect in the root colonization and development of tomato seedlings. *Microorganisms* **8**(**3**):412 DOI 10.3390/microorganisms8030412.

Miethke M, Marahiel MA. 2007. Siderophore-based iron acquisition and pathogen control. *Microbiology and Molecular Biology Reviews* **71**(**3**):413–451 DOI 10.1128/MMBR.00012-07.

Minorsky PV. 2002. Trigonelline: a diverse regulator in plants. *Plant physiology* **128**(**1**):7–8 DOI 10.1104/pp.900014.

Murashige T, Skoog F. 1962. A revised medium for rapid growth and bio assays with tobacco tissue cultures. *Physiologia Plantarum* **15**(**3**):473–497 DOI 10.1111/j.1399-3054.1962.tb08052.x.

O'Sullivan DJ, O'Gara F. 1992. Traits of fluorescent *Pseudomonas* spp. involved in suppression of plant root pathogens. *Microbiological Reviews* **56**(**4**):662–676 DOI 10.1128/MMBR.56.4.662-676.1992.

Pallab M, Shubhasis D, Soumya C, Balaram G, Chiranjit S, Jasmina K, Tapan P. 2019. Simultaneous determination and quantitation of diosmetin and hesperetin in human plasma by liquid chromatographic mass spectrometry with an application to pharmacokinetic studies. *Journal of Chromatographic Science* **57**(**5**):451–461 DOI 10.1093/chromsci/bmz015.

Pari L, Murugan P. 2004. Protective role of tetrahydrocurcumin against erythromycin estolate-induced hepatotoxicity. *Pharmacological Research* **49**(**5**):481–486 DOI 10.1016/j.phrs.2003.11.005.

Park KR, Nam D, Yun HM, Lee SG, Jang HJ, Sethi G, Cho SK, Ahn KS. 2011. β-caryophyllene oxide inhibits growth and induces apoptosis through the suppression of PI3K/AKT/mTOR/S6K1 pathways and ROS-mediated MAPKs activation. *Cancer Letters* **312**(**2**):0–188.

Prasad YU, Alexander I, Regina F, You DG, Dirk W, Patrick G, Hans-Michael H, Mark S, John EL. 2014. The sucrose-trehalose 6-phosphate (Tre6p) nexus: specificity and mechanisms of sucrose signalling by Tre6p. *Journal of Experimental Botany* **64**(**4**):1051–1068.

Ratledge C, Dover LG. 2000. Iron metabolism in pathogenic bacteria. *Annual Review of Microbiology* **54**(**1**):881–941 DOI 10.1146/annurev.micro.54.1.881.

Rogerio AP, Andrade EL, Leite DFP, Figueiredo CP, Calixto JB. 2009. Preventive and therapeutic anti-inflammatory properties of the sesquiterpene α-humulene in experimental airways allergic inflammation. *British Journal of Pharmacology* **158(4)**:1074–1087 DOI 10.1111/j.1476-5381.2009.00177.x.

Rustamova N, Bobakulov K, Begmatov N, Turak A, Yili A, Aisa HA. 2019. Secondary metabolites produced by endophytic *Pantoea ananatis* derived from roots of *Baccharoides anthelmintica* and their effect on melanin synthesis in murine B16 cells. *Natural Product Research* **10**:1–6.

Sayer JM, Emery TF. 1968. Structures of the naturally occurring hydroxamic acids, fusarinines A and B. *Biochemistry* **7(1)**:184–190 DOI 10.1021/bi00841a023.

Schippers BA, Bakker AW, Bakker PAHM. 2003. Interactions of deleterious and beneficial rhizosphere microorganisms and the effect of cropping practices. *Annual Review of Phytopathology* **25(1)**:339–358.

Schrettl M, Bignell E, Kragl C, Sabiha Y, Loss O, Eisendle M, Wallner A, Arst HN, Haynes K, Haas H. 2007. Distinct roles for intra- and extracellular siderophores during *Aspergillus fumigatus* infection. *PLOS Pathogens* **3(9)**:e128 DOI 10.1371/journal.ppat.0030128.

Schwyn B, Neilands JB. 1987. Universal chemical-assay for the detection and determination of siderophores. *Analytical Biochemistry* **160(1)**:47–56 DOI 10.1016/0003-2697(87)90612-9.

Sharma A, Johri BN, Sharma AK, Glick BR. 2003. Plant growth-promoting bacterium *Pseudomonas* sp. strain GRP3 influences iron acquisition in mung bean (*Vigna radiata* L. Wilzeck).. *Soil Biology and Biochemistry* **35(7)**:887–894 DOI 10.1016/S0038-0717(03)00119-6.

Sheng MM, Jia HK, Zhang GY, Zeng LN, Zhang TT, Long YH, Lan J, Hu ZQ, Zeng Z, Wang B, Liu HM. 2020. Siderophore production by rhizosphere biological control bacteria *Brevibacillus brevis* GZDF3 of *Pinellia ternata* and its antifungal effects on *Candida albicans*. *Journal of Microbiology and Biotechnology* **30(5)**:689–699.

Shenker M, Oliver I, Helmann M, Hadar Y, Chen Y. 1992. Utilization by tomatoes of iron mediated by a siderophore produced by *Rhizopus arrhizus*. *Journal of Plant Nutrition* **15(10)**:2173–2182 DOI 10.1080/01904169209364466.

Shi H, Li Y, Li P, Wang Z, Chen S. 2016. Effect of nitrogen-fixing *Paenibacillus* spp.on wheat yield. *Journal of China Agricultural University* **21(6)**:52–55.

Shuangya C, Yongxiang Z, Xiangqun C. 2003. Mechanism of three bacterial strains to inhibit *Stagonospora curtisii* causing leaf spot of Narcissus tazetta. *Chinese Journal of Biological Control* **19(1)**:11–15.

Song G, Luo Q, Qin J, Wang L, Shi Y, Sun C. 2006. Effects of oxymatrine on proliferation and apoptosis in human hepatoma cells. *Colloids and Surfaces B Biointerfaces* **48(1)**:1–5 DOI 10.1016/j.colsurfb.2005.12.012.

Tramontano WA, Jouve D. 1997. Trigonelline accumulation in salt-stressed legumes and the role of other osmoregulators as cell cycle control agents. *Phytochemistry* **44(6)**:1037–1040 DOI 10.1016/S0031-9422(96)00715-7.

Trivedi MK, Gangwar M, Mondal SC, Jana S. 2017. Protective effects of tetrahydrocurcumin (THC) on fibroblast and melanoma cell lines in vitro: it's implication for wound healing. *Journal of Food Science and Technology* **54(5)**:1137–1145 DOI 10.1007/s13197-017-2525-8.

Wang L, Li J, Li Q, Chen S. 2013. *Paenibacillus beijingensis* sp nov.a nitrogen-fixing species isolated from wheat rhizosphere soil. *Antonie van Leeuwenhoek* **105(2)**:675–683.

Weyers JDB, Paterson NW. 2001. Plant hormones and the control of physiological processes. *New Phytologist* **152(3)**:375–407 DOI 10.1046/j.0028-646X.2001.00281.x.

Wingler A, Delatte TL, O"Hara LE, Primavesi LF, Jhurreea D, Schluepmann PH. 2012. Trehalose 6-phosphate is required for the onset of leaf senescence associated with high carbon availability. *Plant Physiology* **158(3)**:1241–1251 DOI 10.1104/pp.111.191908.

Xie B, Xu K, Zhao H, Chen S. 2005. Isolation of transposon mutants from *Azospirillum brasilense* Yu62 and characterization of genes involved in indole-3-acetic acid biosynthesis. *FEMS Microbiology Letters* **248(1)**:57–63 DOI 10.1016/j.femsle.2005.05.020.

Xie J, Shi H, Du Z, Wang T, Liu X, Chen S. 2016. Comparative genomic and functional analysis reveal conservation of plant growth promoting traits in *Paenibacillus polymyxa* and its closely related species. *Scientific Report* **6(1)**:21329 DOI 10.1038/srep21329.

Yahara S, Uda N, Yoshio E, Yae E. 2004. Steroidal alkaloid glycosides from tomato (*Lycopersicon esculentum*). *Journal of Natural Products* **67(3)**:500–502 DOI 10.1021/np030382x.

Yang DP, Michel L, Chaumont JP, Millet-Clerc J. 1999. Use of caryophyllene oxide as an antifungal agent in an in vitro experimental model of onychomycosis. *Mycopathologia* **148(2)**:79–82 DOI 10.1023/A:1007178924408.

Yehuda Z, Shenker M, Romheld V, Marschner H, Chen Y. 1996. The role of ligand exchange in the uptake of iron from microbial siderophores by gramineous plants. *Plant Physiology* **112(3)**:1273–1280 DOI 10.1104/pp.112.3.1273.

Yuquan X, Hong G, Genglei T, Xinde Z. 1999. Siderophore production and their activity against *Piricularia oryzae* by Pseudomonas JKD-2. *Microbiology* **26(3)**:180–183.